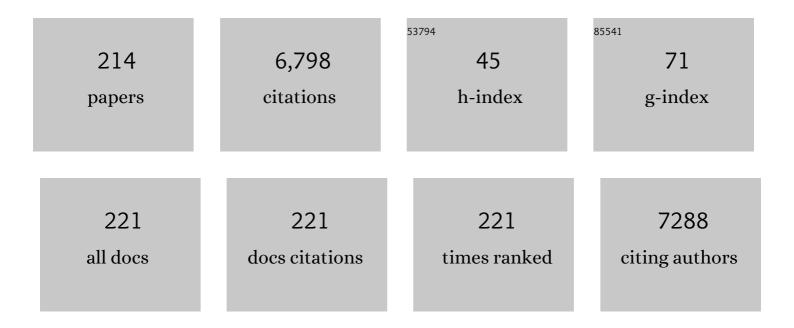
## Ayman nafady

List of Publications by Year in descending order

Source: https://exaly.com/author-pdf/7891655/publications.pdf Version: 2024-02-01



#	Article	IF	CITATIONS
1	Recent advances in MOF-based photocatalysis: environmental remediation under visible light. Inorganic Chemistry Frontiers, 2020, 7, 300-339.	6.0	429
2	A MOFâ€based Ultraâ€Strong Acetylene Nanoâ€trap for Highly Efficient C <sub>2</sub> H <sub>2</sub> /CO <sub>2</sub> Separation. Angewandte Chemie - International Edition, 2021, 60, 5283-5288.	13.8	172
3	Lower Activation Energy for Catalytic Reactions through Host–Guest Cooperation within Metal–Organic Frameworks. Angewandte Chemie - International Edition, 2018, 57, 10107-10111.	13.8	166
4	MnO <sub><i>x</i></sub> Nanoparticle-Dispersed CeO <sub>2</sub> Nanocubes: A Remarkable Heteronanostructured System with Unusual Structural Characteristics and Superior Catalytic Performance. ACS Applied Materials & Interfaces, 2015, 7, 16525-16535.	8.0	154
5	Facile Approach to Graft Ionic Liquid into MOF for Improving the Efficiency of CO <sub>2</sub> Chemical Fixation. ACS Applied Materials & Interfaces, 2018, 10, 27124-27130.	8.0	142
6	Reaction Environment Modification in Covalent Organic Frameworks for Catalytic Performance Enhancement. Angewandte Chemie - International Edition, 2019, 58, 8670-8675.	13.8	128
7	Designing CuO <sub><i>x</i></sub> Nanoparticle-Decorated CeO <sub>2</sub> Nanocubes for Catalytic Soot Oxidation: Role of the Nanointerface in the Catalytic Performance of Heterostructured Nanomaterials. Langmuir, 2016, 32, 2208-2215.	3.5	127
8	Effective and fast adsorptive removal of toxic cationic dye (MB) from aqueous medium using amino-functionalized magnetic multiwall carbon nanotubes. Journal of Molecular Liquids, 2019, 282, 154-161.	4.9	124
9	Ceria–zirconia modified MnO <sub>x</sub> catalysts for gaseous elemental mercury oxidation and adsorption. Catalysis Science and Technology, 2016, 6, 1792-1803.	4.1	122
10	One-Electron Oxidation of Ruthenocene: Reactions of the Ruthenocenium Ion in Gentle Electrolyte Media. Inorganic Chemistry, 2009, 48, 2156-2165.	4.0	118
11	Nanowire Morphology of Mono- and Bidoped α-MnO <sub>2</sub> Catalysts for Remarkable Enhancement in Soot Oxidation. ACS Applied Materials & Interfaces, 2017, 9, 32652-32666.	8.0	116
12	Application of nanotechnology in agriculture, postharvest loss reduction and food processing: food security implication and challenges. Heliyon, 2021, 7, e08539.	3.2	116
13	Synthesis and characterization of new Cr(III), Fe(III) and Cu(II) complexes incorporating multi-substituted aryl imidazole ligand: Structural, DFT, DNA binding, and biological implications. Spectrochimica Acta - Part A: Molecular and Biomolecular Spectroscopy, 2020, 228, 117700.	3.9	107
14	l-cysteine protected copper nanoparticles as colorimetric sensor for mercuric ions. Talanta, 2014, 130, 415-422.	5.5	106
15	Tunable Synthesis of Hollow Metal–Nitrogen–Carbon Capsules for Efficient Oxygen Reduction Catalysis in Proton Exchange Membrane Fuel Cells. ACS Nano, 2019, 13, 8087-8098.	14.6	106
16	Redox Activity and Two-Step Valence Tautomerism in a Family of Dinuclear Cobalt Complexes with a Spiroconjugated Bis(dioxolene) Ligand. Journal of the American Chemical Society, 2013, 135, 8304-8323.	13.7	102
17	Preparation of Metalâ <sup>^,</sup> TCNQ Charge-Transfer Complexes on Conducting and Insulating Surfaces by Photocrystallization. Journal of the American Chemical Society, 2007, 129, 2066-2073.	13.7	98
18	Co <sub>3</sub> O <sub>4</sub> @CeO <sub>2</sub> hybrid flower-like microspheres: a strong synergistic peroxidase-mimicking artificial enzyme with high sensitivity for glucose detection. Journal of Materials Chemistry B, 2017, 5, 720-730.	5.8	96

#	Article	IF	CITATIONS
19	Pore environment engineering in metal–organic frameworks for efficient ethane/ethylene separation. Journal of Materials Chemistry A, 2019, 7, 13585-13590.	10.3	91
20	Characterization of the Successive One-Electron Oxidation Products of the Dicobalt Fulvalenediyl (Fv) Compound Co <sub>2</sub> Fv(CO) <sub>4</sub> and its Phosphine-Substituted Product. Organometallics, 2008, 27, 5624-5631.	2.3	90
21	Nanospace Engineering of Metal–Organic Frameworks through Dynamic Spacer Installation of Multifunctionalities for Efficient Separation of Ethane from Ethane/Ethylene Mixtures. Angewandte Chemie - International Edition, 2021, 60, 9680-9685.	13.8	89
22	Pore surface engineering of covalent organic frameworks: structural diversity and applications. Nanoscale, 2019, 11, 21679-21708.	5.6	82
23	Characterization and Reactions of Previously Elusive 17-Electron Cations:  Electrochemical Oxidations of (C6H6)Cr(CO)3 and (C5H5)Co(CO)2 in the Presence of [B(C6F5)4] Journal of the American Chemical Society, 2002, 124, 7260-7261.	13.7	76
24	Tuning the Electrocrystallization Parameters of Semiconducting Co[TCNQ]2-Based Materials To Yield either Single Nanowires or Crystalline Thin Films. Journal of the American Chemical Society, 2007, 129, 2369-2382.	13.7	75
25	Controlling Core/Shell Formation of Nanocubic <i>p</i> -Cu <sub>2</sub> 0/ <i>n</i> -ZnO Toward Enhanced Photocatalytic Performance. Langmuir, 2015, 31, 10922-10930.	3.5	75
26	[Re(η5-C5H5)(CO)3]+Family of 17-Electron Compounds: Monomer/Dimer Equilibria and Other Reactions. Journal of the American Chemical Society, 2008, 130, 2692-2703.	13.7	69
27	Electrochemical Preparation of the Bis(ruthenocenium) Dication. Inorganic Chemistry, 2003, 42, 5480-5482.	4.0	68
28	Enhancing Photocatalytic Hydrogen Production via the Construction of Robust Multivariate Tiâ€MOF/COF Composites. Angewandte Chemie - International Edition, 2022, 61, .	13.8	67
29	Electrochemical and photochemical routes to semiconducting transition metal-tetracyanoquinodimethane coordination polymers. Coordination Chemistry Reviews, 2014, 268, 101-142.	18.8	66
30	Covalent Organic Framework Decorated with Vanadium as a New Platform for Prins Reaction and Sulfide Oxidation. ACS Applied Materials & amp; Interfaces, 2019, 11, 3070-3079.	8.0	66
31	Glycine-assisted synthesis of NiO hollow cage-like nanostructures for sensitive non-enzymatic glucose sensing. RSC Advances, 2015, 5, 18773-18781.	3.6	62
32	Observation of Ferromagnetic Exchange, Spin Crossover, Reductively Induced Oxidation, and Field-Induced Slow Magnetic Relaxation in Monomeric Cobalt Nitroxides. Inorganic Chemistry, 2013, 52, 7557-7572.	4.0	61
33	Manipulating the Electrolyte Medium to Favor Either One-Electron or Two-Electron Oxidation Pathways for (Fulvalendiyl)dirhodium Complexes. Organometallics, 2006, 25, 1654-1663.	2.3	59
34	Chemical, physical, and biological properties of Pd(II), V(IV)O, and Ag(I) complexes of N <sub>3</sub> tridentate pyridine-based Schiff base ligand. Journal of Coordination Chemistry, 2020, 73, 3150-3173.	2.2	59
35	Electrochemical Oxidation of CoCp(CO)2:Â Radicalâ^'Substrate Reaction of a 17 e-/18 e-Pair and Production of a Unique Dimer Radical. Journal of the American Chemical Society, 2006, 128, 16587-16599.	13.7	57
36	A Porous Organic Polymer Nanotrap for Efficient Extraction of Palladium. Angewandte Chemie - International Edition, 2020, 59, 19618-19622.	13.8	57

#	Article	IF	CITATIONS
37	Catalytic Oxidation of Benzyl Alcohol Using Nanosized Cu/Ni Schiff-Base Complexes and Their Metal Oxide Nanoparticles. Catalysts, 2018, 8, 452.	3.5	56
38	Hollow capsules of doped carbon incorporating metal@metal sulfide and metal@metal oxide core–shell nanoparticles derived from metal–organic framework composites for efficient oxygen electrocatalysis. Journal of Materials Chemistry A, 2019, 7, 3624-3631.	10.3	53
39	Ultra-trace level electrochemical sensor for methylene blue dye based on nafion stabilized ibuprofen derived gold nanoparticles. Sensors and Actuators B: Chemical, 2015, 208, 320-326.	7.8	51
40	The formation of gold nanoparticles using hydroquinone as a reducing agent through a localized pH change upon addition of NaOH to a solution of HAuCl4. Colloids and Surfaces A: Physicochemical and Engineering Aspects, 2010, 370, 35-41.	4.7	50
41	Development of sensitive non-enzymatic glucose sensor using complex nanostructures of cobalt oxide. Materials Science in Semiconductor Processing, 2015, 34, 373-381.	4.0	50
42	Recent advances in preparation methods for catalytic thin films and coatings. Catalysis Science and Technology, 2019, 9, 3582-3602.	4.1	50
43	Chemically and electrochemically induced expansion and contraction of a ferrocene rotor. Chemical Communications, 2015, 51, 8161-8164.	4.1	49
44	Simpler and highly sensitive enzyme-free sensing of urea via NiO nanostructures modified electrode. RSC Advances, 2016, 6, 39001-39006.	3.6	49
45	A MOFâ€based Ultraâ€Strong Acetylene Nanoâ€ŧrap for Highly Efficient C <sub>2</sub> H <sub>2</sub> /CO <sub>2</sub> Separation. Angewandte Chemie, 2021, 133, 5343-5348.	2.0	49
46	Installation of synergistic binding sites onto porous organic polymers for efficient removal of perfluorooctanoic acid. Nature Communications, 2022, 13, 2132.	12.8	49
47	Secondâ€Sphere Interaction Promoted Turnâ€On Fluorescence for Selective Sensing of Organic Amines in a Tb <sup>III</sup> â€based Macrocyclic Framework. Angewandte Chemie - International Edition, 2021, 60, 23705-23712.	13.8	48
48	Vanadium Docked Covalent-Organic Frameworks: An Effective Heterogeneous Catalyst for Modified Mannich-Type Reaction. ACS Sustainable Chemistry and Engineering, 2019, 7, 4878-4888.	6.7	46
49	Morphology Changes and Mechanistic Aspects of the Electrochemically-Induced Reversible Solidâ^`Solid Transformation of Microcrystalline TCNQ into Co[TCNQ]2-Based Materials (TCNQ =) Tj ETQq1 1 0.	78 <b>4637</b> 14 rg	BT4®verlock
50	Mercury Sorption and Desorption on Gold: A Comparative Analysis of Surface Acoustic Wave and Quartz Crystal Microbalance-Based Sensors. Langmuir, 2015, 31, 8519-8529.	3.5	43
51	Tranexamic acid derived gold nanoparticles modified glassy carbon electrode as sensitive sensor for determination of nalbuphine. Sensors and Actuators B: Chemical, 2015, 211, 359-369.	7.8	42
52	Sensitive and selective aggregation based colorimetric sensing of Fe3+ via interaction with acetyl salicylic acid derived gold nanoparticles. Sensors and Actuators B: Chemical, 2018, 259, 1006-1012.	7.8	42
53	Non-Linear Optical Property and Biological Assays of Therapeutic Potentials Under In Vitro Conditions of Pd(II), Ag(I) and Cu(II) Complexes of 5-Diethyl amino-2-({2-[(2-hydroxy-Benzylidene)-amino]-phenylimino}-methyl)-phenol. Molecules, 2020, 25, 5089.	3.8	42
54	3D Cationic Polymeric Network Nanotrap for Efficient Collection of Perrhenate Anion from Wastewater. Small, 2021, 17, e2007994.	10.0	42

#	Article	IF	CITATIONS
55	Voltammetric, Spectroscopic, and Microscopic Investigations of Electrocrystallized Forms of Semiconducting AgTCNQ (TCNQ = 7,7,8,8-Tetracyanoquinodimethane) Exhibiting Different Morphologies and Colors. Chemistry of Materials, 2007, 19, 5499-5509.	6.7	40
56	Reaction Environment Modification in Covalent Organic Frameworks for Catalytic Performance Enhancement. Angewandte Chemie, 2019, 131, 8762-8767.	2.0	40
57	Chemical composition and Biological studies of Ficus benjamina. Chemistry Central Journal, 2014, 8, 12.	2.6	39
58	Synthesis, Characterization, Theoretical Studies, and Antimicrobial/Antitumor Potencies of Salen and Salen/Imidazole Complexes of Co (II), Ni (II), Cu (II), Cd (II), Al (III) and La (III). Applied Organometallic Chemistry, 2020, 34, e5912.	3.5	39
59	Detailed Electrochemical Analysis of the Redox Chemistry of Tetrafluorotetracyanoquinodimethane TCNQF4, the Radical Anion [TCNQF4]•–, and the Dianion [TCNQF4]2–in the Presence of Trifluoroacetic Acid. Analytical Chemistry, 2011, 83, 6731-6737.	6.5	38
60	Green Synthesis of AgNPs <sup>()</sup> Ultilizing <i>Delonix Regia</i> Extract as Anticancer and Antimicrobial Agents**. ChemistrySelect, 2020, 5, 13263-13268.	1.5	38
61	Anion Dependent Redox Changes in Iron Bis-terdentate Nitroxide {NNO} Chelates. Inorganic Chemistry, 2011, 50, 3052-3064.	4.0	37
62	Anodic Preparation of [Re2Cp2(CO)6]2+:Â A Dimeric Dication that Provides the Powerful One-Electron Oxidant [ReCp(CO)3]+. Journal of the American Chemical Society, 2005, 127, 15676-15677.	13.7	34
63	Efficient Electron Transfer from Electronâ€Sponge Polyoxometalate to Singleâ€Metal Site Metal–Organic Frameworks for Highly Selective Electroreduction of Carbon Dioxide. Small, 2021, 17, e2100762.	10.0	34
64	Lower Activation Energy for Catalytic Reactions through Host–Guest Cooperation within Metal–Organic Frameworks. Angewandte Chemie, 2018, 130, 10264-10268.	2.0	33
65	Cefuroxime derived copper nanoparticles and their application as a colorimetric sensor for trace level detection of picric acid. RSC Advances, 2016, 6, 82882-82889.	3.6	30
66	Electrospun carbon nanofiber-encapsulated NiS nanoparticles as an efficient catalyst for hydrogen production from hydrolysis of sodium borohydride. International Journal of Hydrogen Energy, 2019, 44, 21716-21725.	7.1	30
67	Structural modifications in Co–Zn nanoferrites by Gd substitution triggering to dielectric and gas sensing applications. Journal of Alloys and Compounds, 2020, 844, 156178.	5.5	30
68	Nanostructured Co3O4 electrocatalyst for OER: The role of organic polyelectrolytes as soft templates. Electrochimica Acta, 2021, 398, 139338.	5.2	30
69	NiCo2O4 nanostructures loaded onto pencil graphite rod: An advanced composite material for oxygen evolution reaction. International Journal of Hydrogen Energy, 2022, 47, 6650-6665.	7.1	30
70	Redox-Induced Solidâ^'Solid Phase Transformation of TCNQ Microcrystals into Semiconducting Ni[TCNQ]2(H2O)2Nanowire (Flowerlike) Architectures:Â A Combined Voltammetric, Spectroscopic, and Microscopic Study. Inorganic Chemistry, 2007, 46, 4128-4137.	4.0	29
71	Structural, spectroscopic, FMOs, and non-linear optical properties exploration of three thiacaix(4)arenes derivatives. Arabian Journal of Chemistry, 2022, 15, 103656.	4.9	29
72	Recent Advances in Mesoporous Silica Nanoparticles for Targeted Drug Delivery Applications. Current Drug Delivery, 2022, 19, 436-450.	1.6	28

#	Article	IF	CITATIONS
73	Electrode Kinetics Associated with Tetracyanoquinodimethane (TCNQ), TCNQ <sup>•–</sup> , and TCNQ <sup>2–</sup> Redox Chemistry in Acetonitrile As Determined by Analysis of Higher Harmonic Components Derived from Fourier Transformed Large Amplitude ac Voltammetry. Journal of Physical Chemistry C, 2011, 115, 24153-24163.	3.1	27
74	Voltammetric reduction and re-oxidation of solid coordination polymers of dihydroxybenzoquinone. Chemical Communications, 2012, 48, 11422.	4.1	27
75	Cotton cloth supported tungsten carbide/carbon nanocomposites as a Janus film for solar driven interfacial water evaporation. Journal of Materials Chemistry A, 2021, 9, 23140-23148.	10.3	26
76	Fabrication of Er, Tb doped CuO thin films using nebulizer spray pyrolysis technique for photosensing applications. Optical Materials, 2022, 123, 111954.	3.6	26
77	Controllable Synthesis and Fabrication of Semiconducting Nanorod/Nanowire Bundles of Fe[TCNQ] <sub>2</sub> (H <sub>2</sub> O) <sub>2</sub> via Electrochemically Induced Solidâ Solid Phase Transformation of TCNQ Microcrystals. Journal of Physical Chemistry C, 2008, 112, 6700-6709.	3.1	25
78	Fabrication of oxidized graphite supported La2O3/ZrO2 nanocomposite for the photoremediation of toxic fast green dye. Journal of Molecular Liquids, 2019, 277, 738-748.	4.9	25
79	Singleâ€Pore versus Dualâ€Pore Bipyridineâ€Based Covalent–Organic Frameworks: An Insight into the Heterogeneous Catalytic Activity for Selective CH Functionalization. Small, 2021, 17, e2003970.	10.0	25
80	Two step synthesis of TiO2–Co3O4 composite for efficient oxygen evolution reaction. International Journal of Hydrogen Energy, 2021, 46, 9110-9122.	7.1	25
81	Utilization of cationic microporous metal-organic framework for efficient Xe/Kr separation. Nano Research, 2022, 15, 7559-7564.	10.4	25
82	Hyperelectronic Metalâ^'Carborane Analogues of Cymantrene (MnCp(CO) <sub>3</sub> ) Anions: Electronic and Structural Noninnocence of the Tricarbadecaboranyl Ligand. Organometallics, 2007, 26, 4471-4482.	2.3	24
83	Iridium complex immobilization on covalent organic framework for effective C—H borylation. APL Materials, 2019, 7, .	5.1	24
84	Design, synthesis and molecular modeling of novel aryl carboximidamides and 3-aryl-1,2,4-oxadiazoles derived from indomethacin as potent anti-inflammatory iNOS/PGE2 inhibitors. Bioorganic Chemistry, 2020, 105, 104439.	4.1	24
85	Preparation and thermoelectric power properties of highly doped p-type Sb2Te3 thin films. Physica E: Low-Dimensional Systems and Nanostructures, 2021, 127, 114505.	2.7	23
86	Redox and Acid–Base Chemistry of 7,7,8,8-Tetracyanoquinodimethane, 7,7,8,8-Tetracyanoquinodimethane Radical Anion, 7,7,8,8-Tetracyanoquinodimethane Dianion, and Dihydro-7,7,8,8-Tetracyanoquinodimethane in Acetonitrile. Analytical Chemistry, 2012, 84, 2343-2350.	6.5	22
87	Cu <sub>2</sub> <sup>I</sup> (TCNQF <sub>4</sub> <sup>Ilâ€"</sup> )(MeCN) <sub>2</sub> (TCNQF <sub>4</sub> = 2,3,5,6-Tetrafluoro-7,7,8,8-tetracyanoquinodimethane): Voltammetry, Simulations, Bulk Electrolysis, Spectroscopy, Photoactivity, and X-ray Crystal Structure of the Cu <sub>2</sub> <sup>I</sup> (TCNOF <sub>4</sub> <sup>Ilâ€"</sup> )(EtCN) <sub>2</sub> Analogue.	4.0	22
88	Inorganic Chemistry, 2014, 53, 3230-3242 Cellulose acetate nanofibers embedded with Ag nanoparticles/CdSe/graphene oxide composite for degradation of methylene blue. Synthetic Metals, 2021, 278, 116824.	3.9	22
89	Design and fabrication of green and sustainable vapochromic cellulose fibers embedded with natural anthocyanin for detection of toxic ammonia. Talanta, 2021, 230, 122292.	5.5	22
90	Catalytic Reductive Degradation of Methyl Orange Using Air Resilient Copper Nanostructures. Journal of Nanomaterials, 2015, 2015, 1-12.	2.7	21

#	Article	IF	CITATIONS
91	Easy, one-step synthesis of CdTe quantum dots via microwave irradiation for fingerprinting application. Materials Research Bulletin, 2017, 90, 260-265.	5.2	21
92	Biogenic Silver Nanoparticles for Trace Colorimetric Sensing of Enzyme Disrupter Fungicide Vinclozolin. Nanomaterials, 2019, 9, 1604.	4.1	21
93	Ranolazine-Functionalized Copper Nanoparticles as a Colorimetric Sensor for Trace Level Detection of As3+. Nanomaterials, 2019, 9, 83.	4.1	21
94	Synthesis of Co(OH) <sub>2</sub> /CNTs nanocomposite with superior rate capability and cyclic stability for energy storage applications. Materials Research Express, 2020, 7, 125501.	1.6	21
95	Scalable and low-cost fabrication of flexible WS2 photodetectors on polycarbonate. Npj Flexible Electronics, 2022, 6, .	10.7	21
96	AFM study of morphological changes associated with electrochemical solid–solid transformation of three-dimensional crystals of TCNQ to metal derivatives (metal = Cu, Co, Ni;) Tj ETQq0 0 0 rgBT /Overlo	ck2 <b>1.0</b> Tf 5	0 52307 Td (TC
97	Direct synthesis and stabilization of Bi-sized cysteine-derived gold nanoparticles: Reduction catalyst for methylene blue. Journal of the Iranian Chemical Society, 2011, 8, S34-S43.	2.2	20
98	The facile assembly of bis-, tris- and poly(triazaphosphole) systems using "click―chemistry. Dalton Transactions, 2013, 42, 7775.	3.3	20
99	Functional Porphyrinic Metal–Organic Framework as a New Class of Heterogeneous Halogenâ€Bondâ€Donor Catalyst. Angewandte Chemie - International Edition, 2021, 60, 24312-24317.	13.8	20
100	New Family of Ferric Spin Clusters Incorporating Redox-Active <i>ortho</i> -Dioxolene Ligands. Inorganic Chemistry, 2009, 48, 7765-7781.	4.0	19
101	Fabrication and Applications of Potentiometric Sensors Based on p-tert-butylthiacalix[4]arene Comprising Two Triazole Rings Ionophore for Silver Ion Detection. International Journal of Electrochemical Science, 2016, , 4729-4742.	1.3	19
102	Crystalline and porous CoSe dendrimeric architectures for efficient oxygen evolution reaction. Fuel, 2022, 323, 124324.	6.4	19
103	Silver/gold core/shell nanowire monolayer on a QCM microsensor for enhanced mercury detection. RSC Advances, 2015, 5, 92303-92311.	3.6	18
104	Highly sensitive determination of atropine using cobalt oxide nanostructures: Influence of functional groups on the signal sensitivity. Analytica Chimica Acta, 2016, 948, 30-39.	5.4	18
105	CoCr 7 C 3 -like nanorods embedded on carbon nanofibers as effective electrocatalyst for methanol electro-oxidation. International Journal of Hydrogen Energy, 2018, 43, 9943-9953.	7.1	18
106	Microporous Cyclen-Based Octacarboxylate Hydrogen-Bonded Organic Framework Exhibiting Selective Gas Adsorption. Crystal Growth and Design, 2019, 19, 6377-6380.	3.0	18
107	Heterotrimetallic Ru(II)/Pd(II)/Ru(II) complexes: Synthesis, crystalstructure, spectral characterization, DFT calculation and antimicrobial study. Spectrochimica Acta - Part A: Molecular and Biomolecular Spectroscopy, 2014, 122, 273-282.	3.9	17
108	Cobalt nanoparticles incorporated into hollow doped porous carbon capsules as a highly efficient oxygen reduction electrocatalyst. Catalysis Science and Technology, 2018, 8, 5244-5250.	4.1	17

#	Article	IF	CITATIONS
109	Mechanical and thermoelectric properties of FeVSb-based half-Heusler alloys. Journal of Alloys and Compounds, 2021, 886, 161308.	5.5	17
110	Electrochemistry of the bis(1,4,7-triazacyclodecane) cobalt(III) complex and its role in the catalytic reduction of hydrogen. Polyhedron, 1998, 17, 4535-4541.	2.2	16
111	A systematic study of the variation of tetrathiafulvalene (TTF), TTF <sup>+</sup> Ë™ and TTF <sup>2+</sup> reaction pathways with water in the presence and absence of light. RSC Advances, 2014, 4, 49789-49795.	3.6	16
112	An amperometric sensitive dopamine biosensor based on novel copper oxide nanostructures. Microsystem Technologies, 2017, 23, 1229-1235.	2.0	16
113	Fabrication of Highly Sensitive and Selective Electrochemical Sensors for Detection of Paracetamol by Using Piroxicam Stabilized Gold Nanoparticles. Journal of the Electrochemical Society, 2017, 164, B427-B434.	2.9	16
114	Enzymes and phytochemicals from neem extract robustly tuned the photocatalytic activity of ZnO for the degradation of malachite green (MG) in aqueous media. Research on Chemical Intermediates, 2021, 47, 1581-1599.	2.7	16
115	Strongly Anisotropic Strainâ€Tunability of Excitons in Exfoliated ZrSe <sub>3</sub> . Advanced Materials, 2022, 34, e2103571.	21.0	16
116	Ni Nanoparticles Embedded Ti3C2Tx-MXene Nanoarchitectures for Electrochemical Sensing of Methylmalonic Acid. Biosensors, 2022, 12, 231.	4.7	16
117	Electrochemical Synthesis and Characterization of Semiconducting Ni(TCNQF4)2(H2O)2 (TCNQF4 =) Tj ETQq1 2 2012, 2889-2897.	1 0.78431 2.0	4 rgBT /Ov€r 15
118	Novel Cr (III), Fe (III) and Ru (III) Vanillin Based Metalloâ€Pharmaceuticals for Cancer and Inflammation Treatment: Experimental and Theoretical Studies. Applied Organometallic Chemistry, 2019, 33, e5177.	3.5	15
119	Facile NiCo2S4/C nanocomposite: an efficient material for water oxidation. Tungsten, 2020, 2, 403-410.	4.8	15
120	A window-space-directed assembly strategy for the construction of supertetrahedron-based zeolitic mesoporous metal–organic frameworks with ultramicroporous apertures for selective gas adsorption. Chemical Science, 2021, 12, 5767-5773.	7.4	15
121	Facile fabrication of Fe-BDC/Fe-2MI heterojunction with boosted photocatalytic activity for Cr(VI) reduction. Journal of Environmental Chemical Engineering, 2021, 9, 105961.	6.7	15
122	Enhancing Photocatalytic Hydrogen Production via the Construction of Robust Multivariate Tiâ€MOF/COF Composites. Angewandte Chemie, 2022, 134, .	2.0	15
123	Electrochemically-Induced TCNQ/Mn[TCNQ] <sub>2</sub> (H <sub>2</sub> O) <sub>2</sub> (TCNQ =) Tj ETQq1	1 0.7843	14 rgBT /Ove 14
120	Processes That Allow Selective Generation of Nanofiber or Nanorod Network Morphologies. Inorganic Chemistry, 2009, 48, 9258-9270.		
124	A flow cell for transient voltammetry and in situ grazing incidence X-ray diffraction characterization of electrocrystallized cadmium(II) tetracyanoquinodimethane. Electrochimica Acta, 2011, 56, 1546-1553.	5.2	14
125	A ferrocenyl-substituted 1,2,4-triazole ligand and its Fell, Nill and Cull 1D-chain complexes. Dalton Transactions, 2013, 42, 10326.	3.3	14
126	Low Temperature Aqueous Chemical Growth Method for the Doping of W into ZnO Nanostructures and Their Photocatalytic Role in the Degradration of Methylene Blue. Journal of Cluster Science, 2022, 33, 1445-1456.	3.3	14

#	Article	IF	CITATIONS
127	Effects of spark plasma sintering on enhancing the thermoelectric performance of Hf–Ti doped VFeSb half-Heusler alloys. Journal of Physics and Chemistry of Solids, 2021, 150, 109848.	4.0	13
128	Antibacterial potency, cell viability and morphological implications of copper oxide nanoparticles encapsulated into cellulose acetate nanofibrous scaffolds. International Journal of Biological Macromolecules, 2021, 182, 464-471.	7.5	13
129	Eco-Friendly Disposable WS2 Paper Sensor for Sub-ppm NO2 Detection at Room Temperature. Nanomaterials, 2022, 12, 1213.	4.1	13
130	Substitution of CO Ligand by P(OPh)3 in Radical Cations of the Cymantrene Family: Relationships of Substitution Rates to E1/2 Values and Carbonyl IR Frequencies. Journal of Inorganic and Organometallic Polymers and Materials, 2014, 24, 137-144.	3.7	12
131	Voltammetric studies on the inter-relationship between the redox chemistry of TTF, TTF <sup>+</sup> Ë™, TTF <sup>2+</sup> and HTTF <sup>+</sup> in acidic media. RSC Advances, 2015, 5, 18384-18390.	3.6	12
132	Ascorbic Acid Assisted Synthesis of Cobalt Oxide Nanostructures, Their Electrochemical Sensing Application for the Sensitive Determination of Hydrazine. Journal of Electronic Materials, 2016, 45, 3695-3701.	2.2	12
133	Silky Co <sub>3</sub> O <sub>4</sub> nanostructures for the selective and sensitive enzyme free sensing of uric acid. RSC Advances, 2021, 11, 5156-5162.	3.6	12
134	Facile Electrochemical Determination of Methotrexate (MTX) Using Glassy Carbon Electrode-Modified with Electronically Disordered NiO Nanostructures. Nanomaterials, 2021, 11, 1266.	4.1	12
135	Highly selective, sensitive and simpler colorimetric sensor for Fe2+ detection based on biosynthesized gold nanoparticles. Spectrochimica Acta - Part A: Molecular and Biomolecular Spectroscopy, 2021, 254, 119645.	3.9	12
136	Electrochemical studies with dissolved and surface-confined forms of neo-pentyl-ferrocene-based polyesters utilising [NBu4][B(C6F5)4] and other electrolytes. Journal of Solid State Electrochemistry, 2009, 13, 1511-1519.	2.5	11
137	Construction of an Ultrasensitive and Highly Selective Nitrite Sensor Using Piroxicam-Derived Copper Oxide Nanostructures. Catalysts, 2018, 8, 29.	3.5	11
138	Optical properties of thin Bi2Te3 films synthesized by different techniques. Superlattices and Microstructures, 2021, 155, 106909.	3.1	11
139	Anodic Reaction of Co(η <sup>5</sup> -C <sub>5</sub> H <sub>5</sub> )(CO)(PPh <sub>3</sub> ): An Oxidatively Induced Ligand Exchange Involving a 17 e <sup>â^²</sup> /18 e <sup>â^²</sup> Redox Pair. Organometallics, 2010, 29, 4276-4281.	2.3	10
140	Characterization of Newly Synthesized ZrFe2O5Nanomaterial and Investigations of Its Tremendous Photocatalytic Properties under Visible Light Irradiation. Journal of Nanomaterials, 2013, 2013, 1-6.	2.7	10
141	Role of Water in the Dynamic Disproportionation of Zn-Based TCNQ(F4) Coordination Polymers (TCNQ) Tj ETQq1	1,0,7843 4.0	14 rgBT /O
142	Catalytic degradation of imidacloprid using L-serine capped nickel nanoparticles. Materials Express, 2015, 5, 121-128.	0.5	10
143	A new sensitive electrochemical method for the determination of vanadium(IV) and vanadium(V) in Benfield sample. Talanta, 2015, 132, 541-547.	5.5	10
144	A Porous Organic Polymer Nanotrap for Efficient Extraction of Palladium. Angewandte Chemie, 2020, 132, 19786-19790.	2.0	10

#	Article	IF	CITATIONS
145	Utilization of hybrid silicone rubber/Exolit AP 422 composite for the fabrication of mechanically flexible, flame-retardant and superhydrophobic polyurethane foams. Materials Chemistry and Physics, 2021, 273, 125133.	4.0	10
146	Electrochemically Directed Synthesis of Co <sup>2+</sup> and Ni <sup>2+</sup> Complexes with TCNQF <sub>4</sub> <sup>2–</sup> (TCNQF <sub>4</sub> =) Tj ETQq0 0 0 rgBT /Overlock 10 Tf 50 702 To	l (2,3,5,6â€ 2.0	Tetrafluoroâ€
147	2012, 5534-5541. Nanospace Engineering of Metal–Organic Frameworks through Dynamic Spacer Installation of Multifunctionalities for Efficient Separation of Ethane from Ethane/Ethylene Mixtures. Angewandte Chemie, 2021, 133, 9766-9771.	2.0	9
148	Electrochemical sensing of dopamine via bio-assisted synthesized silver nanoparticles. International Nano Letters, 2021, 11, 263-271.	5.0	9
149	Two Manganese Metalloporphyrin Frameworks Constructed from a Custom-Designed Porphyrin Ligand Exhibiting Selective Uptake of CO <sub>2</sub> over CH <sub>4</sub> and Catalytic Activity for CO <sub>2</sub> Fixation. Crystal Growth and Design, 2021, 21, 2786-2792.	3.0	9
150	Aggregation of a Dibenzo[ <i>b</i> , <i>def</i> ]chrysene Based Organic Photovoltaic Material in Solution. Journal of Physical Chemistry B, 2014, 118, 6839-6849.	2.6	8
151	Metal–Organic Charge Transfer Complexes of Pb(TCNQ) 2 and Pb(TCNQF 4 ) 2 as New Catalysts for Electron Transfer Reactions. Advanced Materials Interfaces, 2020, 7, 2001111.	3.7	8
152	Synthesis, structural characterization, and biological studies of ATBS–M complexes (M(II) = Cu, Co e2000241.	, Ni,) Tj ETQ 4.1	q0 0 0 rgBT /C 8
153	Development of silk fibers decorated with the in situ synthesized silver and gold nanoparticles: antimicrobial activity and creatinine adsorption capacity. Journal of Industrial and Engineering Chemistry, 2021, 97, 584-596.	5.8	8
154	A simple and efficient visible light photodetector based on Co3O4/ZnO composite. Optical and Quantum Electronics, 2021, 53, 1.	3.3	8
155	Secondâ€Sphere Interaction Promoted Turnâ€On Fluorescence for Selective Sensing of Organic Amines in a Tb <sup>III</sup> â€based Macrocyclic Framework. Angewandte Chemie, 2021, 133, 23898-23905.	2.0	8
156	Kinetic and thermodynamic interplay of cation ingress and egress at a TCNQ-modified electrode in contact with aqueous electrolyte mixtures containing Co(II) and Ni(II) cations. Journal of Solid State Electrochemistry, 2013, 17, 1609-1620.	2.5	7
157	Solid-State Electrochemistry of a Semiconducting MMX-Type Diplatinum Iodide Chain Complex. Inorganic Chemistry, 2014, 53, 4022-4028.	4.0	7
158	Conditions Favoring the Formation of Monomeric Pt <sup>III</sup> Derivatives in the Electrochemical Oxidation of <i>trans</i> â€{Pt <sup>II</sup> {( <i>p</i> â€BrC <sub>6</sub> F <sub>4</sub> )NCH <sub>2</sub> CH <sub>2&lt; ChemElectroChem, 2015, 2, 1048-1061.</sub>	/sub <sup>3</sup> NEt <s< td=""><td>sub<sup>7</sup>2}(</td></s<>	sub <sup>7</sup> 2}(
159	Investigation of the Anticancer Activity of Coordination-Driven Self-AssembledTwo-Dimensional Ruthenium Metalla-Rectangle. Molecules, 2019, 24, 2284.	3.8	7
160	Enhanced desalination process using a Cu–ZnO-polyvinyl chloride-nylon nanofiltration membrane as a calcite antiscalant in reverse osmosis. Materials Express, 2020, 10, 671-679.	0.5	7
161	The Synthesis of New Nanostructures of CuO Using Ascorbic Acid as Growth Directing Agent and Their Sensitive Electrochemical Detection of Hydrazine. Sensor Letters, 2016, 14, 611-615.	0.4	7
162	Microwave-assisted synthesis of L-cysteine-capped nickel nanoparticles for catalytic reduction of 4-nitrophenol. Rare Metals, 2015, 34, 683-691.	7.1	6

#	Article	IF	CITATIONS
163	Electrochemistry with the extremely weak coordinating anions: Using of carboranes [H-CB11X6Y5]â^' (X) Tj ETQq 755, 1-6.	1 1 0.784 3.8	314 rgBT /C 6
164	Ultraâ€sensitive Amperometric Hydrazine Sensing via Dimethyl Glyoxomat Derived NiO Nanostructures. Electroanalysis, 2017, 29, 2803-2809.	2.9	6
165	Trace Level Colorimetric Hg2+ Sensor Driven by Citrus japonica Leaf Extract Derived Silver Nanoparticles: Green Synthesis and Application. Journal of Cluster Science, 2022, 33, 1865-1875.	3.3	6
166	Stretching ReS2 along different crystal directions: Anisotropic tuning of the vibrational and optical responses. Applied Physics Letters, 2022, 120, .	3.3	6
167	Pd-Co3O4-based nanostructures for the development of enzyme-free glucose sensor. Bulletin of Materials Science, 2022, 45, 1.	1.7	6
168	Neo-Pentyl-Ferrocene Based Electroactive Polyesters. Journal of Inorganic and Organometallic Polymers and Materials, 2008, 18, 485-490.	3.7	5
169	Mechanistic Pathways and Identification of the Electrochemically Generated Oxidation Products of Flavonoid Eriodictyol in the Presence of Glutathione. Electroanalysis, 2018, 30, 1714-1722.	2.9	5
170	Fabrication of FeO(OH)/CNTs composite based electrode with self-supporting and flexible design for foldable hybrid capacitors. Ceramics International, 2021, 47, 34881-34890.	4.8	5
171	Preferential synthesis of highly conducting Tl(TCNQ) phase II nanorod networks via electrochemically driven TCNQ/Tl(TCNQ) solid-solid phase transformation. Journal of Solid State Electrochemistry, 2016, 20, 3303-3314.	2.5	4
172	Sub-ppt level voltammetric sensor for Hg2+ detection based on nafion stabilized l-cysteine-capped Au@Ag core-shell nanoparticles. Journal of Solid State Electrochemistry, 2019, 23, 2073-2083.	2.5	4
173	Antimycobacterial, Antioxidant and Cytotoxicity Activities of Mesoporous Nickel Oxide Nanoparticles for Healthcare. Coatings, 2020, 10, 1242.	2.6	4
174	Co2+ Substituted Spinel MgCuZn Ferrimagnetic Oxide: A Highly Versatile Electromagnetic Material via a Facile Molten Salt Route. Nanomaterials, 2020, 10, 2333.	4.1	4
175	Synthesis of Sheet Like Nanostructures of NiO Using Potassium Dichromate as Surface Modifying Agent for the Sensitive and Selective Determination of Amlodipine Besylate (ADB) Drug. Electroanalysis, 2021, 33, 1121-1128.	2.9	4
176	Increased Crystallization of CuTCNQ in Water/DMSO Bisolvent for Enhanced Redox Catalysis. Nanomaterials, 2021, 11, 954.	4.1	4
177	Paper-supported WS2 strain gauges. Sensors and Actuators A: Physical, 2021, 332, 113204.	4.1	4
178	The fast nucleation/growth of Co <sub>3</sub> O <sub>4</sub> nanowires on cotton silk: the facile development of a potentiometric uric acid biosensor. RSC Advances, 2022, 12, 18321-18332.	3.6	4
179	Copper vanadate nanowires-based MIS capacitors: synthesis, characterization, and their electrical charge storage applications. Journal of Nanoparticle Research, 2013, 15, 1.	1.9	3
180	Design, Synthesis, Characterization of Novel Ruthenium(II) Catalysts: Highly Efficient and Selective Hydrogenation of Cinnamaldehyde to (E)-3-Phenylprop-2-en-1-ol. Molecules, 2014, 19, 5965-5980.	3.8	3

#	Article	IF	CITATIONS
181	Synthesis and characterization of microstructured sheets of semiconducting Ca[TCNQ]2 via redox-driven solid-solid phase transformation of TCNQ microcrystals. Journal of Solid State Electrochemistry, 2014, 18, 851-859.	2.5	3
182	Fabrication of Fe-POMs as Visible-light-active Heterogeneous Photocatalyst. Chemical Research in Chinese Universities, 2020, 36, 1128-1135.	2.6	3
183	Efficient and Stable Co3O4/ZnO Nanocomposite for Photochemical Water Splitting. Journal of Cluster Science, 2022, 33, 387-394.	3.3	3
184	Fabrication of Hybrid Materials Based on Waste Polyethylene/Porous Activated Metakaolinite Nanocomposite as an Efficient Membrane for Heavy Metal Desalination Processes. Adsorption Science and Technology, 2021, 2021, 1-15.	3.2	3
185	Chemically Coupled Cobalt Oxide Nanosheets Decorated onto the Surface of Multiwall Carbon Nanotubes for Favorable Oxygen Evolution Reaction. Journal of Nanoscience and Nanotechnology, 2021, 21, 2660-2667.	0.9	3
186	Manipulation of optical properties in thin tetradymite layers. Optical Materials, 2021, 115, 111026.	3.6	3
187	New Quinoline-2-one/thiazolium bromide Derivatives; Synthesis, Characterization and Mechanism of Formation. Journal of Molecular Structure, 2021, 1239, 130501.	3.6	3
188	Structural, Spectroscopic, and Electrochemical Characterization of Semi-Conducting, Solvated [Pt(NH3)4](TCNQ)2·(DMF)2 and Non-Solvated [Pt(NH3)4](TCNQ)2. Australian Journal of Chemistry, 2017, 70, 997.	0.9	2
189	The Crystal Disorder into ZnO with Addition of Bromine and It's Outperform Role in the Photodegradation of Methylene Blue. Journal of Cluster Science, 2022, 33, 281-291.	3.3	2
190	TiO2/ZnO Nanocomposite Material for Efficient Degradation of Methylene Blue. Journal of Nanoscience and Nanotechnology, 2021, 21, 2511-2519.	0.9	2
191	Covalent–Organic Frameworks: Singleâ€Pore versus Dualâ€Pore Bipyridineâ€Based Covalent–Organic Frameworks: An Insight into the Heterogeneous Catalytic Activity for Selective CH Functionalization (Small 22/2021). Small, 2021, 17, 2170109.	10.0	2
192	Flower-like CuO/polyaniline composite for electrochemical determination of hydrochlorothiazide. Bulletin of Materials Science, 2021, 44, 1.	1.7	2
193	Cephradine-Capped Gold Nanoparticle Modified Glassy Carbon Electrode for Trace Level Sensing of Triphenyltin Hydroxide. Journal of the Electrochemical Society, 2020, 167, 137503.	2.9	2
194	Voltammetric behavior of microparticles and thin films of neo-pentyl-ferrocene-based polyester (PmFB): Manipulation of anion uptake at the ionic liquid/aqueous electrolyte interface. Electrochemistry Communications, 2009, 11, 1838-1841.	4.7	1
195	A Combined Voltammetric and Synchrotron Radiation-Grazing Incidence X-ray Diffraction Study of the Electrocrystallization of Zinc Tetracyanoquinodimethane. Australian Journal of Chemistry, 2012, 65, 236.	0.9	1
196	Novel Semiconducting Biomaterials Derived from a Proline Ester and Tetracyanoquinodimethane Identified by Handpicked Selection of Individual Crystals. Australian Journal of Chemistry, 2012, 65, 935.	0.9	1
197	Frontispiz: Reaction Environment Modification in Covalent Organic Frameworks for Catalytic Performance Enhancement. Angewandte Chemie, 2019, 131, .	2.0	1
198	Chemically Coupled Multiwall Carbon Nanotubes with Leaf-Like Nanostructures of NiO for Sensitive and Selective Determination of Uric Acid. Journal of Electronic Materials, 2021, 50, 2852-2859.	2.2	1

#	Article	IF	CITATIONS
199	Frontispiz: A MOFâ€based Ultra‣trong Acetylene Nanoâ€trap for Highly Efficient C <sub>2</sub> H <sub>2</sub> /CO <sub>2</sub> Separation. Angewandte Chemie, 2021, 133, .	2.0	1
200	Carbon Dioxide Electroreduction: Efficient Electron Transfer from Electronâ€Sponge Polyoxometalate to Singleâ€Metal Site Metal–Organic Frameworks for Highly Selective Electroreduction of Carbon Dioxide (Small 20/2021). Small, 2021, 17, 2170095.	10.0	1
201	Polyaniline as a sacrificing template for the synthesis of controlled Co3O4 nanoparticles for the sensitive and selective detection of methotrexate (MTX). Journal of Materials Science: Materials in Electronics, 2021, 32, 15594-15604.	2.2	1
202	Strongly Anisotropic Strainâ€Tunability of Excitons in Exfoliated ZrSe <sub>3</sub> (Adv. Mater. 1/2022). Advanced Materials, 2022, 34, .	21.0	1
203	Efficient Adsorption of Carbofuran via Tailored Porous Polyacrylonitrile Film Incorporating Ti-MIL Coordination Polymer. Journal of Inorganic and Organometallic Polymers and Materials, 2022, 32, 1409-1421.	3.7	1
204	Role of cobalt precursors in the synthesis of <scp> Co <sub>3</sub> O <sub>4</sub> </scp> hierarchical nanostructures toward the development of cobaltâ€based functional electrocatalysts for bifunctional water splitting in alkaline and acidic media. Journal of the Chinese Chemical Society, 0, , .	1.4	1
205	Crystal structure of 2-phenoxyethyl 2-hydroxybenzoate, C15H14O4. Zeitschrift Fur Kristallographie - New Crystal Structures, 2014, 229, .	0.3	0
206	Frontispiece: Reaction Environment Modification in Covalent Organic Frameworks for Catalytic Performance Enhancement. Angewandte Chemie - International Edition, 2019, 58, .	13.8	0
207	Rücktitelbild: A Porous Organic Polymer Nanotrap for Efficient Extraction of Palladium (Angew.) Tj ETQq1 1 0.7	784314 rg 2.0	BT/Overlock
208	Frontispiece: A MOFâ€based Ultraâ€Strong Acetylene Nanoâ€trap for Highly Efficient C <sub>2</sub> H <sub>2</sub> /CO <sub>2</sub> Separation. Angewandte Chemie - International Edition, 2021, 60, .	13.8	0
209	MoSx–Co3O4 Nanocomposite for Selective Determination of Ascorbic Acid. Journal of Nanoscience and Nanotechnology, 2021, 21, 2595-2603.	0.9	0
210	Cationic Polymeric Networks: 3D Cationic Polymeric Network Nanotrap for Efficient Collection of Perrhenate Anion from Wastewater (Small 20/2021). Small, 2021, 17, 2170094.	10.0	0
211	Synthesis of composite material of cobalt oxide (Co3O4) with hydroxide functionalized multi-walled carbon nanotubes (MWCNTs) for electrochemical determination of uric acid. Journal of Materials Science: Materials in Electronics, 2021, 32, 20047-20057.	2.2	0
212	Facile Co 3 O 4 nanoparticles deposited on polyvinylpyrrolidine for efficient water oxidation in alkaline media. Journal of the Chinese Chemical Society, 0, , .	1.4	0
213	Utilization of polyvinyl amine hydrolysis product in enhancing the catalytic properties of Co3O4 nanowires: toward potentiometric glucose bio-sensing application. Journal of Materials Science: Materials in Electronics, 0, , 1.	2.2	0
214	Innenrücktitelbild: Enhancing Photocatalytic Hydrogen Production via the Construction of Robust Multivariate Tiâ€MOF/COF Composites (Angew. Chem. 3/2022). Angewandte Chemie, 2022, 134, .	2.0	0